Slurry Jet Erosion Test Rig: A Review of Erosive Particles Induction Methods and Its Test Parameters

S. Karthik[1] · **H. J. Amarendra**[1]

Abstract

Slurry erosion as problem was identified during World War II in oil and munitions industries. Industrial components were severely damaged due to interaction with fluid and particles inclusion, resulted in huge financial losses. To evaluate the erosion, slurry erosion test set-ups were developed. In this article, slurry jet erosion test set-ups developed are reviewed and are classified based on the erosive particles induction method. Each test set-ups are named after the initial test set-up originators, namely Levy, Turenne, Hutchings, and Thapa test method, respectively. Test set-ups are further categorized into premixing and postmixing type and recirculation and non-recirculation of slurry type. For each test method, number of researchers adopted the test method and number of research articles published by the researchers are illustrated. Emphases are made on the erosion test parameters viz velocity, nozzle diameter, concentration, and erosive particles type and size. From the literature, it is observed that Turenne test method is the most popular test method, while Levy test method is the less popular method; based on adoption of test method by the researchers. For the test parameters, Thapa method is with high velocity (117.3 m/s) while Hutchings method is with low velocity (1.5 m/s) and Hutchings method is with high concentration (40 wt%) while Thapa method is with the lowest concentration (0.0015 wt%).

Keywords Slurry jet erosion test set-up · Velocity · Concentration · Nozzle · Erosive particles

List of Symbols

v	Velocity (m/s)
d	Nozzle diameter (mm)
C	Slurry concentration, weight (wt) %
p	Erosive particle type
s	Erosive particle size (μm)
M	Materials evaluated (SS, stainless steel; *SMM*, surface modified materials; Al, aluminum; CI, cast iron; G, glass; ce, cement; E, epoxy based mortar; MMCs, metal matrix composites; WC, tungsten carbide; Co, cobalt; Ti, titanium; Cu, copper; HEA, high entropy alloy; Al_2O_3, aluminum oxide, Alumina; GFRP, glass fiber-reinforced plastic composites; Zr, zirconia; NAB, nickel–aluminum–bronze; SMA, shape memory alloy)

✉ S. Karthik
 mechkarth@gmail.com

1 Department of Mechanical Engineering, Malnad College of Engineering, Hassan, affiliated to VTU, Belagavi, Karnataka, India

1 Introduction

Erosion as a problem was identified during the World War II, when damage to the industrial equipments was observed in Australia [1] and Germany [2]. Professor Finnie from USA, earliest one to provoked the interest into erosion research, noticed the degradation of materials in industrial applications like sand blast, abrasive deburring, and drilling processes. Introduction of catalytic cracking process by 1942 further stepped up the erosion of oil industry components [3]. Contemporarily, Professor Philip Bowden, Consultant for Shell Oil Company, UK, noticed the damage on the munitions industry components of Australia by erosion. He pointed that the reasons for the components damage as friction [5], damage due to liquid impact at high speeds [6], and the particles inclusion effect on the damage was also of his keen interest [7].

Industrial components were falling well short before their expected life and research is carried to identify reasons for the early failure [1]. Similar consequences were also observed in industries such as steam turbines, rocket nozzles, and aerospace industries [8, 9]. Early research was pertaining with the erosion of components, and reports about

erosion as a problem were described, but the basic understanding received meager attention [10]. Earlier researchers were unable to believe that the damage of components was due to particle inclusions, that too in reducing their life severely [11]. Researchers from versatile backgrounds engaged themselves to study the erosion by building the test set-up and evaluation of the materials, suitable for their applications, either by identifying the use of certain materials with better properties or by modifying the material with suitable techniques [12–15], but the erosion was there to occur on those materials as well. Finnie estimated the loss for the oil industry in the USA was about $5000 per annum during 1957 by erosion [4]. About 300,000 British pounds incurred only for replacement of offshore oil industry valves, and the damage in these industries is dominated by erosion [16]. Huge financial loss incurred due to erosion across fluids handling and processing industries all across the globe and went unnoticed before the significant emphasis on erosion [17–19].

Materials to be used as industrial components were evaluated for its erosion resistance, for which, variety of erosion test set-ups were used [20–23]. The researchers devised the erosion test set-ups for the operational requirements. Two types of erosion measuring approaches have been employed, first, the pipe wear testing (real conditions, as in industries) and second, laboratory tests (scaled down). Former method is most preferred, as it is more economical both in time and capital cost [24]. Three types of laboratory erosion test set-ups were commonly used to evaluate the materials erosion. They are slinger type, rotating type and the jet erosion test set-ups. In slinger type, multiple specimens were located on the surface of the chamber filled with slurry, rotating drum will carry the slurry to impact on the specimens [25]. In rotating type test set-ups, specimens were mounted on the arm of a shaft, rotates in the vertical plane. Slurry filled in the container impinges on the specimens fixed on the arm [26]. In above two cases, slurry rather than impacting on material was glazing/sliding along their surface, through which the impact characteristics of the erosive particles were found to be unknown. The jet erosion test set-ups permit variation of number of test parameters viz impingement angle, velocity, nozzle diameter, and concentration and significantly provides to evaluate the test materials under pure impact conditions. This system uses pressurized gas/water jet with erosive particles [27, 28].

Many slurry jet erosion test set-ups were developed and used to evaluate the materials erosion resistance/behavior under various slurry erosive conditions. Figure 1 is the geographical indicator shows the countries involved in building slurry jet test set-ups for erosion research. Chronological order 1 indicates first test set-up developed, and 11 indicates last test set-up contributor found from literature. The number of test set-ups developed in the representative nation is shown besides.

In this article, slurry jet erosion test set-ups built, rebuilt, and used by researchers to evaluate the erosion characteristics of the materials are reviewed. Of the slurry jet test set-ups found, based on the erosive particles induction method, categorized into premixing and postmixing of erosive particles and recirculation (RC) and non-recirculation (NRC) of slurry type. All the test set-ups are derived under four common test methods, namely, Levy, Turenne, Hutchings, and Thapa test methods. Test parameters like velocity, nozzle diameter, particle kinetic energy, concentration, and erosive particles type and size are compared individually for each test methods and at later stage, all the test methods are put together and compared for high and low velocity and high and low concentration test set-up.

Country - No. of test rigs
1 - USA - 2
2 - Canada - 3
3 - UK - 8
4 - South Africa - 3
5 - Singapore - 2
6 - Japan - 2
7 - Nepal - 2
8 - Taiwan - 1
9 - India - 5
10 - Colombia - 2
11 - China - 3

Fig. 1 Geographical indicator of slurry jet erosion test set-ups built across the globe

2 Classification of Test Set-Ups

2.1 Test Set-Up Type

Slurry jet erosion test set-up is widely used, as it provides flexibility in operating parameters. For better understanding, the test set-ups are divided into two broad categories, namely,

(1) re-circulation (RC) and nonrecirculation (NRC) of slurry.
(2) premix and postmixing of slurry (pressurizing the fluid with or without erosive particles).

Erosive particles if reused are categorized as recirculation type, as erosive particles are recirculated throughout the testing cycle. In this category, the erosive particles will damage the pump components. While in non-recirculation type, erosive particles are used only once.

2.2 Test Methods

From the literature, numerous slurry jet test set-ups are found, but it was very cumbersome to advance for the review of test set-ups before simplifying the approach. Therefore,

the authors narrowed down and classified the test set-ups based on the erosive particle induction method into the driving fluid. Four common test methods are drawn out, their schematic are shown in Fig. 2a–d. The literature shows that the latter researchers have modified/altered the test set-ups keeping the basic concept intact.

Figure 2a shows the first conceptual approach called as Levy test method. Water and kerosene were used as the fluids. Known quantity of erosive particles such as coal, aluminum oxide (Al_2O_3), and silicon carbide (SiC) is added to the container meanwhile stirred by the stirrer. Slurry in the container is pressurized by gas or air, carried through the nozzle to impinge on the material [28]. Figure 2b shows the Turenne test method. Turenne test set-up is incorporated with air-powered slurry pump to pump the premixed quantity of erosive particles added to the fluid forming the slurry mixture [29]. Figure 2c represents the Hutchings test method. Test set-up was provided with a multistage pump to drive the fluid, water. An ejector assembly is positioned along the main flow line to entrain the slurry mixture stored in a tank. A low pressure region is created due to differential cross section at the driving and driven nozzle in the ejector. This low pressure helps to suck the slurry in to the main flow line [30]. Last test method is the Thapa test method shown in Fig. 2d. Thapa test set-up was provided with a centrifugal pump to drive
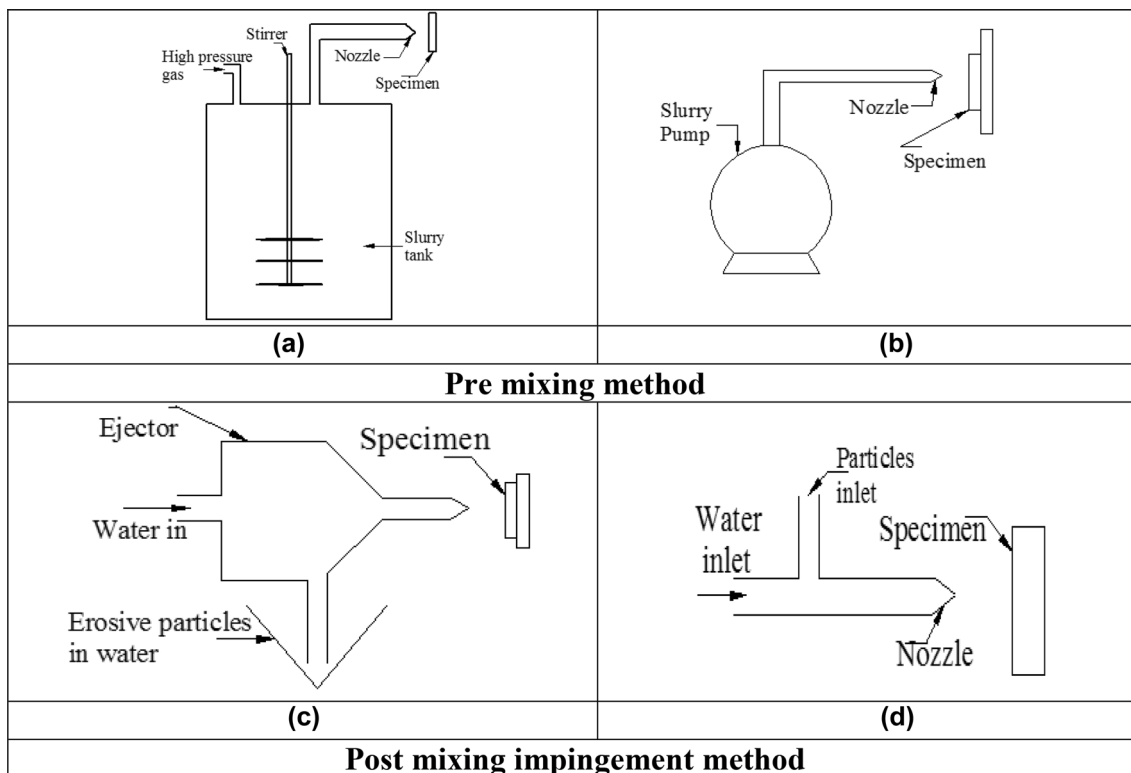

Fig. 2 Slurry jet erosion test methods

the water. A hopper located along the main flow line is loaded with erosive particles. Erosive particles entry is regulated by varying the orifice opening by the valve. Flow of water causes disturbance to the erosive particles in the hopper and falls into the main flow line due to gravity [31].

Based on the classification of test method, a pie chart is drawn as shown in Fig. 3 to show adoptability of test methods by the researchers. It can be observed that Turenne test method is the most popular test method while Levy test method is less popular.

2.3 Test Parameters

Erosion evaluation depends on material, erosive particles, fluid medium, and flow parameters, and it increases further by the synergetic effects. Properties of materials such as composition, hardness, fatigue, and tensile strength etc., the use of surface modified and coated materials add to the complexity. Properties of erosive particles are its type, density, hardness, shape, size, etc. Fluid properties are fluid viscosity, density, corrosivity, etc. Test parameters are flow type, angle of impingement, velocity, kinetic energy, and concentration. With all these associated factors, the erosion evaluation has been a tedious task. Then coming researchers were under dilemma to adopt the previous test methods, as many of the earlier reports doesn't provided the necessary data to reproduce, and further loud the trouble as the rebuilt test set-up didn't yield the prior results [11].
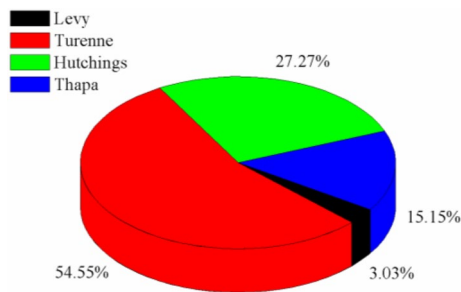

Fig. 3 Test method adopted by researchers

3 Description of Test Methods

Test set-ups developed under each method are tabulated sequentially based on first research article by researchers along with their geographical details, number of research articles published, and the test conditions employed for erosion evaluation and are described in this section.

3.1 Levy Test Method

Levy et al. from the USA in 1980 built the slurry jet erosion test set-up to evaluate the materials' erosion for coal liquefaction industries [28]. This test method is categorized as premixing type and is NRC type. In this test set-up, variation in velocity is achieved by varying the gas regulator pressure. Literature reveals that Levy test method is used only by the original researchers and has not shown its footprint anywhere else in the future research but in University Berkeley Laboratory, USA. The author draws down the following reasons for the same:

- non-availability of the test set-up,
- unable to develop the similar set-up,
- complexity in developing the similar set-up,
- may be it has not created any interest.

Test conditions employed by Levy et al. are illustrated in Table 1.

3.2 Turenne Test Method

Turenne et al. from Canada in 1989 have developed a laboratory slurry jet erosion test set-up [29]. Turenne test method falls under the category of RC and premixing type. Basic principle adopted under this method is to pump the water and erosive particles mixture through the pump to cause erosion on the materials. Commonly used pumps are slurry pump and centrifugal pump. Erosive particles are the agents which induce erosion, through the energy carried by the particles in the fluid. In order to achieve increase in concentration, some researchers have used a stirrer in their test set-up [34, 81, 98]. Santa et al. modified centrifugal pump exit such

Table 1 Test conditions under Levy test method

Author	References	Test conditions					
		v	d	C	p	s	M
Levy, USA	[28]	12, 15, 18, 21, 23, 27, 30, 33, 38	3	10, 20, 30	Coal, SiC, Al$_2$O$_3$	24, 150	Cu, Al, MS
	[32]	8, 15, 17, 21, 22, 23	3	20	Coal, SiC, Al$_2$O$_3$	24, 150	Cu, Al, MS
	[33]	10, 12, 20, 30	3	30	Coal, sand	150	Steel, SS
	[34]	12, 23, 30	5	0.12, 0.24	Sand	355–710	Steel

that to locate the material at the exit to provide grazing incidence [79]. Grewal et al. have used two pumps, main pump to drive water and other to pump the slurry [87]. Nguyen et al. have used peristaltic pump to pump the slurry [99]. Water is used as driving fluid in all test set-ups developed by the researchers but Santa et al. only one to use distilled water as driving fluid. Yoganandh et al. have used the test set-up developed by Ducom Instruments. Table 2 illustrates the research articles published and the test conditions with which the researchers evaluated the materials' erosion under Turenne test method. In the Turenne test method, it can be noticed that, for pumping the premixed slurry into the test chamber, the components of the pump used are susceptible to erosion in turn reducing their performance efficiency.

Kinetic energy plays an important role in the erosion of materials, because erosion relies on the kinetic energy that the erosive particles possess. It is directly proportional to the square of the velocity indicates that increase in kinetic energy results in increase in erosion and vice versa. Amount of erosion caused depends on the materials hardness. Under Turenne test method, Wood et al. have evaluated the materials at kinetic ranges from 0.017 to 8 μJ. Higher the kinetic energy of the particles, higher is the erosion [63]. Similar approach was adopted by Sugiyama et al., in which erosion evaluation was conducted on SS material. It is observed that, at lesser kinetic energies (< 1 μJ), there was no erosion occurred, as the kinetic energy increased from > 1 μJ, the erosion was occurred and as the energy increases (upto 15 μJ), the erosion of the SS material got increased [70]. The kinetic energy values achieved by Wood and Sugiyama et al. are mentioned in Table 2. No kinetic energy values are found from other researchers under Turenne test method.

3.3 Hutchings Test Method

Hutchings et al. from United Kingdom in 1990 have developed a laboratory slurry jet erosion test set-up [30]. This test method is an interdependent type test method, and velocity and concentration depend on diameter ratio of driver (*d*) to driven nozzle (*D*) of ejector. In this test set-up, velocity increases with increase in *d*/*D* ratio while concentration decreases with increase in *d*/*D* ratio. Slurry after impacting the material will fall back to the slurry tank, and then recirculated through ejector. In this test set-up, driving fluid alone is driven by the pump, while the erosive particles are drawn into the main flow line only through the ejector. Unlike in Turenne test method, rather than pumping the slurry into the test chamber this test method utilizes ejector, which overcomes the erosion of pump components. Test set-up built by Hutchings has been modified by keeping ejector principle intact to evaluate erosion and erosion corrosion by using certain add-ons like electrochemical cell, electrodes [105–108]. This test method is categorized as postmixing and of recirculating type (RC). To homogenize

the erosive particles and water, stirrer was used in the Zhang test set-up. Driving fluid used is water for slurry erosion test. For synergy of erosion corrosion water, sometimes distilled water with suitable chemicals/solutions was used to induce corrosion environment [109]. Table 2 illustrates the test conditions adopted by researchers in their research article under Hutchings test method.

Kinetic energy values under Hutchings test method is mentioned only by Wood et al., which varies from 0.016 to 0.41 μJ. Wood et al. have evaluated the materials' erosion under both Turenne and Hutchings test method. It can be noticed that kinetic energy values under Turenne test method was ranging from 0.017 to 8 μJ, but while Hutchings test method is used, its value ranges from 0.016 to 0.41 μJ. The velocity under Turenne test method was varied from 4.7 to 28 m/s while in Hutchings test method, it varied from 3.1 to 6.7 m/s, which indicates that higher the velocity, higher the kinetic energy. No kinetic energy values are found from other researchers under Hutchings test method (Table 3).

3.4 Thapa Test Method

Bhola Thapa et al. from Nepal in 1999 have developed a laboratory test set-up [31]. Thapa test method falls under the category of postmixing and nonrecirculation type (NRC). Significant importance of this test method is the erosive particles induction into high-pressure fluid flow zone. Under this method, John Sandstorm et al. have used particle injection pump to induct erosive particles, in which the particles are pumped through hydraulic cylinders [131]. Two researchers have not provided details about the principle they adopted for erosive particle induction. Table 4 illustrates the test conditions adopted by the researchers under Thapa test method.

Thapa et al. have built two test set-ups, named as Thapa 1 and Thapa 2. Working principle involved in the first test set-up is described earlier in Sect. 2.2, while in the second test set-up, they have used 2 hoppers placed one below the other. The lower hopper filled with water, while in the upper hopper, the particles are stored, regulated by valve, and will fall to the lower hopper filled with water and are then carried by the driving fluid to the test chamber [Thapa 2] [31]. Lin et al. and Santa et al. have not mentioned the principle they employed for the erosive particles induction. But they have presented the schematic which represents that they attempted the particles induction into the high velocity stream [80, 132].

4 Comparison of the Test Parameters for the Classified Test Methods

Based on the earlier classification at the Sect. 2.2, velocity adopted by researchers across all the classified test methods is shown in Fig. 4. It is clear from the velocity

Table 2 Test conditions under Turenne test method

Author	References	Test conditions						
		v	d	C	p	s	M	E
Turenne, Canada	[29]	17	4.76	1, 5, 10, 15, 20	Silica	200–300	Al, G	–
	[35]	18.5		20	Silica	212–300	Ce, E	
	[36]	15		10	Silica	106, 180–300, 600	Al, MMCs	
	[37]	15		10	Silica	106, 180–300, 600	Al, MMCs	
	[38]	13, 17		1, 10	Silica	180–300	Al	
Neville, UK	[39]	25	–	0.1	Silica	–	SS	
	[40]	25	–	0.1	Silica	–	CI, SS	
	[41]	25	4[a]	0.1	Silica	251–485	SS	
	[42]	17	4[a]	0.08	Silica	–	SS, SMM	
	[43]	17	1.5, 4[a]	0.01, 0.05	Silica	180	Co alloy	
	[44]	17	4[a]	0.01, 0.02, 0.05, 0.09	Silica	180	SS	
	[45]	17	4[a]	0.05	Silica	180	Ti	
	[46]	17	4[a]	0.05	Silica	180	Co alloy, SS	
	[47]	17	4[a]	0.05, 0.1	SiC	180	Ti	
	[48]	17	4[a]	0.05	Silica	180	Co alloy, CI	
	[49]	17	4[a]	0.02, 0.04, 0.06	Silica	180	SS	
	[50]	17	4[a]	0.01, 0.02, 0.03, 0.04, 0.05	Silica	180	SS	
	[51]	17	–	0.02, 0.05	Silica	180	SMM	
	[52]	17	4[a]	0.005, 0.01, 0.02, 0.03, 0.04, 0.05, 0.06, 0.08, 0.09, 0.1	Silica	150–300	SS	
	[53]	17	–	0.02, 0.05, 0.1	Silica	250–300	SS, SMM	
	[54]	17	–	0.02, 0.05	Silica	180	Co Alloy, SS	
	[55]	17	–	0.02, 0.05, 0.1	Silica	250–300	SMM	
	[56]	7, 20	4[a]	0.005, 0.05	Silica	150–300	SS	
	[57]	14	7[a]	1, 5	Silica	212–300	SMM	
	[58]	14	7[a]	0.01, 0.05	Silica	212–300	MMC, SMM	
	[59]	5, 10, 14	7[a]	0.01, 0.05	Silica	200–300	MMC, SMM	
Iwai, Japan	[60]	9, 10, 11, 13, 15, 23	3	0.5, 3.7	Silica	42, 91, 323	SS	
Wood, UK	[61]	4.7, 10, 20	6	2.1	Quartz	62	SS, SMM	0.07, 0.49, 3
	[62]	16.5, 28.5	6	2.1	Quartz	135, 235	WC, SMM	0.5, 7.5
	[63]	10, 16.5, 20, 28.5	6	2.1	Quartz	62, 135, 216, 235	SS, SMM	0.017, 0.07, 0.17, 0.48, 0.7, 8
	[64]	16, 28	6	2.1	Quartz	135, 235	SS, SMM	0.5, 7.5
	[65]	16, 28	6	2.1	Quartz	135, 235	SS, SMM	
Dallaire, Canada	[66]	10	–	15	Quartz	212–300	SMM	
	[67]	13	5	15	Quartz	212–300	SMM	
Sugiyama, Japan	[68]	10, 16, 30, 40	3	1		40	SS, SMM	–
	[69]	10	3	1	Silica	80	Al, Cu, SS, CI	–
	[70]	20, 40	3	1	Silica, Sand	30, 60	SS	1.62, 2.86, 4.99, 8.74, 15

Table 2 (continued)

Author	References	Test conditions						
		v	d	C	p	s	M	E
Machio, South Africa	[71]	12.5	12.5	5	Silica		SMM	
	[72]	12.6	12.5	5	Silica		SMM	
Mann, India	[73]	18.2	6	2.5	Sand	225	SS, Ti, SMM	
	[74]	29	4	7.5	Sand	180–250	SS, SMM	
	[75]	29	4	2.5	Sand	88–177	SS, SMM	
Kamaraj, India	[76]	12	6	1	Silica	< 150, 150–300	SS, SMM	
	[77]	8, 12, 16, 20	6	10	Silica	100	SS, SMM	
	[78]	12	6	1	Silica	100, 375	SS, SMM	
Santa, Colombia	[79]	5.5	NA	10	Quartz	212–300	SS, SMM	
	[80]	10	NA	10	Quartz	212–300	SS, SMM	
Gant, UK	[81]	20	5	5, 10	Silica	180–250	WC–Co	
	[82]	19.9	5	10	Silica	180–250	WC	
	[83]	19.9	5	25	Silica	212–300	WC	
Liu, China	[84]	46	6	3	Quartz	400–625	SMM	
Mohapatra, India	[85]	30, 50, 70	8	3	Sand	75–350	SS, SMM	
Grewal, India	[86]	20, 40, 60	8	0.5, 1, 1.5	Sand	68, 155, 252	SS, SMM	
	[87]	25	4	0.25, 0.5	Sand	< 300	Al, CI	
	[88]	4, 16	4	0.1, 0.5	Sand	< 300	SMM	
	[89]	4, 16	4	0.1, 0.5	Sand	< 300	SS	
	[90]	16	4	0.1	Sand	< 300	SS, SMM	
	[91]	16	4	0.01, 0.1, 0.5	Sand	< 300	Al, CI, SS, SMM	
	[92]	16	4	0.5	Sand	< 300	SS, SMM	
	[93]	4	4	0.1, 0.5	Sand	< 300	SS, SMM	
Yoganandh, India	[94]	25, 30, 35		1, 2, 3	Silica	600	CI	
	[95]	15, 18, 21, 24		3	Silica	600	CI	
	[96]	15, 18, 21, 24		3	Silica	600	CI	
	[97]	24, 26, 28, 30		3	Silica	600	CI, SS	
Nguyen, Singapore	[98]	15, 20, 25, 30	6.4	0.5	Al_2O_3	150	SS	
	[99]	10, 15, 20, 25, 30	6.4	0.5	Al_2O_3	150–180	SS	
	[100]	30	6.4	0.5	Sand	50, 80, 150, 350, 450, 750	SS	
Jun Yao, China	[101]	20		0.2, 0.15, 0.07	Quartz, Sand	180, 250, 300	SS	
	[102]	20		0.2, 0.07	Quartz, Sand	180	SS	
	[103]	20.5		0.5	Silica, Sand	180, 250, 300	SS	
Zhao, China	[104]	10	8	1, 3	Sand	400–1190	HEA	

[a]Dual nozzle test set-up

plot that Hutchings test method is the low velocity test method, while Thapa test method is the high velocity test method. It is also observed from the figure that most of the researchers from all the test methods have evaluated the materials well within 20 m/s velocity except Thapa test method. From literature, materials' erosion with velocity > 6 m/s is termed as high velocity erosion, lesser are low velocity erosion [140, 141]. Hydraulic turbines are operated with velocity of > 100 m/s [136], majority of the test set-ups developed with Thapa method have evaluated

Table 3 Test conditions under Hutchings test method

Author	References	Test conditions						
		v	d	C	p	s	M	E
Hutchings, UK	[30]	5, 5.3, 7.7	4.5, 5, 5.5, 6, 6.5	4.5, 17, 19.2	Silica	600–1000	Al, Cu, MS, Al$_2$O$_3$	
	[110]	4.5	5.5	19.2	Silica	700	Al	
	[108]	3.6	5.5	2	Silica	600–850	Al	
	[111]	3.6	5.5	15	Silica	600–850	Al	
A Ball, South Africa	[109]	11	–	12	Silica	500	Al, MMC, steel	
	[112]	8.5	4.5	10	Silica	500	Al, MMC	
Sullivan, Singapore	[113]	6.6	6	16.2	Sand	850–1180	GFRP	
Allen, South Africa	[105]	7		6.3	Silica	500	WC	
	[114]	6.4		16	Silica	500	WC	
Burstein, UK	[115]	3.8	–	13.2	Sand	425–600	SS	
	[116]	3.8	4.5	13.2	Silica	400–650	SS	
Fang, UK	[117]	7.3	3.7	5	Silica	600–850	SiC, Sialon, Al$_2$O$_3$, Zr	
	[118]	7.3	3.7	5	Silica	600–850	SiC, Sialon, Al$_2$O$_3$, Zr	
	[119]	7.3	3.7	3, 5, 7.5	Silica	600–850	SiC, Sialon, Al$_2$O$_3$, Zr	
	[120]	7.3	3.7	5.6	SiC	600–850	MMC	
	[121]	7.3	–	5	Silica	600–850	Zr	
Wood, UK	[106]	3		5	Silica	820	SS, SMM	
	[122]	3.1, 5, 6, 6.7	–	3	Silica	–	Cu, steel, NAB	0.016, 0.04, 0.09, 0.23, 0.33, 0.41
	[123]	3.1, 5, 6.7	5.5	3	Silica	135, 235	Steel, NAB, SMM	0.02, 0.09, 0.23, 0.41
	[124]	3.1, 5, 6.7	5.5	3	Silica	135, 235	Steel, NAB, SMM	0.02, 0.09, 0.23, 0.41
	[125]	3.1, 5, 6		–	Silica	135, 235	NAB	0.02, 0.04, 0.23, 0.33
Stack, UK	[107]	4.4, 7, 9.2	4	4	Alumina	710	Fe	
	[126]	2, 4		4, 6, 8	Silica	50–250	MS, SMM	
	[127]	2.5, 3.5, 4.5	–	40	Silica	600–710	Steel	
	[128]	2.5, 3.5, 4.5			Al$_2$O$_3$	600–710	Steel	
Zhang, Canada	[129]	1.5, 3, 5		0.1, 0.5, 1, 3	Silica	100	Al	
	[130]	3			Silica	50–250	SMM	

for hydraulic applications, hence to achieve the higher velocity was the researchers' motive [137].

Figure 5 shows the comparison plot of nozzle diameters in the test set-ups. Decrease in nozzle diameter results in increase in velocity and vice versa. With the use of lower diameter nozzle, velocity achieved is high, which necessitates the use of large capacity pumps [87]. Velocity achieved by researchers depends majorly on the type of pump used and on nozzle employed. Variation in velocity with the test set-up is achieved through the use of suitable nozzles. Kinetic energy is also depends velocity, higher the velocity, higher the kinetic energy leads to higher energy of the particles results in increase in materials erosion. Velocity in Thapa test method is higher, but the concentration of erosive particles is less,however, the erosion caused on the materials is high, since energy of the particles is high.

Figure 6 shows the concentration comparative plot. It is observed that Stack et al. under Hutchings test method have reached higher concentration compared with all other test methods, while Thapa test method is low concentration test set-up. Stack et al. under Hutchings test method is classified as high concentration test set-up. From Figs. 4 and 6, it is observed that velocity and concentration are interdependent. As Thapa test method is with high velocity, but with very less concentration compared with other test methods, whereas Hutchings method is classified as low velocity test method and is producing higher concentration.

Concentration attained in the Levy and Turenne test method is high, as the majority of researchers could able to achieve high concentration compared to all other test methods, as they have premixed the particles with the fluid and pumped through pump, but for postmixing type test set-ups, viz Hutchings and Thapa test methods, In Hutchings test

Table 4 Test conditions under Thapa test method

Author	References	Test conditions						
		v	d	C	p	s	M	E
Thapa, Nepal	[31]	50	8	0.28	Sand, garnet, Al$_2$O$_3$	150, 250, 250–500	SS, SMM	–
	[133]	–	–	–	–	212–300, 300–425	SS	–
	[134]	–	–	–	–	212–300, 300–425	SS	–
	[135]	–	–	–	–	–	SS	–
Lin, Taiwan	[132]	74, 83, 91, 100	4	0.015–0.025	Quartz	263–363	SS, SMA	–
	[136]	45	4	0.018–0.022	Quartz	263–363	SMA, SMM	–
	[137]	83, 91, 100, 105, 117.3	4	0.015–0.025	Quartz	263–363	SS, SMM	–
Sandstrom, USA	[131]	21, 31, 61	3	2	SiC	35, 41	WC, steel	–
Thapa, Nepal	Thapa 2 [31]	22, 30, 40, 51, 53, 55, 60, 70, 75, 80	8	0.38, 0.07, 0.08, 0.1, 0.12, 0.15, 0.2	Sand, garnet, Al$_2$O$_3$	150, 250, 250–500	SS, SMM	–
Santa, Colombia	[80]	75	5	0.4	Silica	212–300	SMM	–
	[138]	25	4	0.1	Silica	212–425	SMM	–
	[139]	25	4	0.1	Silica	212–425	SMM	–

Fig. 4 Velocity comparison plot
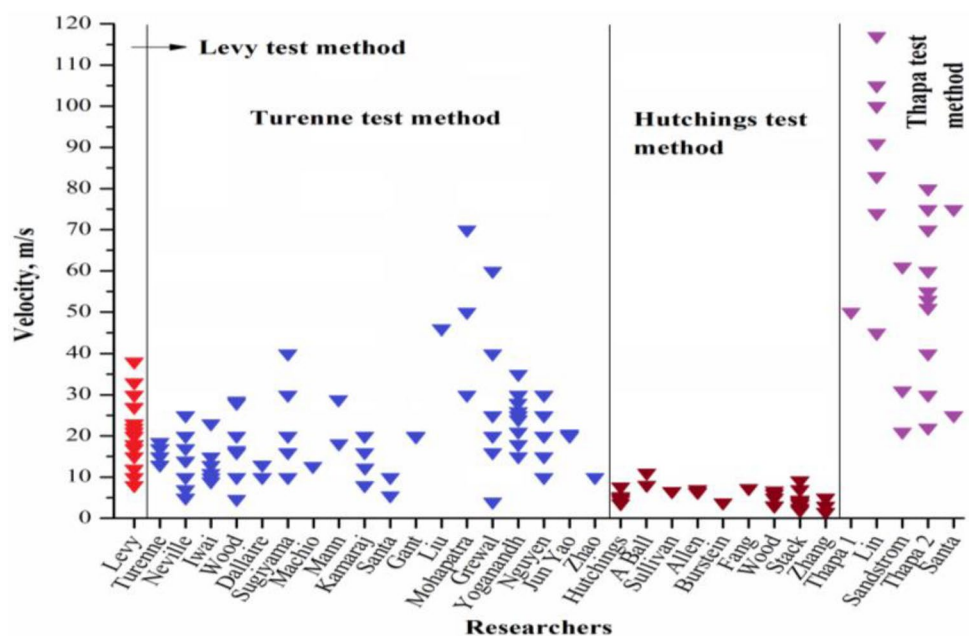
method, the concentration attained depends on the ejector's driving and driven nozzle diameter ratio. Due to the differential cross section of the ejector, negative pressure is created, through which the slurry is sucked. While in Thapa test method, the particles are made to fall due to gravity into the main flow line, and the method involves various conditions to be met up, as the driving fluid passing in the flow line will enter the particles entry passage which obstructs the flow of particles.

It is observed that concentration of particles in the fluid depends on the type of industries. Concentration in the fluid reaches about 1–2 wt%, and the hydraulic turbines will shut down [142],for offshore applications, the high concentration observed is about 0.01 wt% [65]. Likewise to deal with the erosion in various industries, researchers built the test setups to suite for their particular application.

Under Turenne test method, majority of the research carried is concerned with hydraulic industries, as five test setups were developed to evaluate material for its applications [68, 76, 79, 85, 87]. Next major research is on material used for offshore gate valve applications, two test set-ups were developed [61, 73], later, each test set-ups were developed to investigate the material for sewage, sludge pump [60], and for nuclear industries application [101],, respectively. Jet

Fig. 5 Nozzle diameter comparison plot
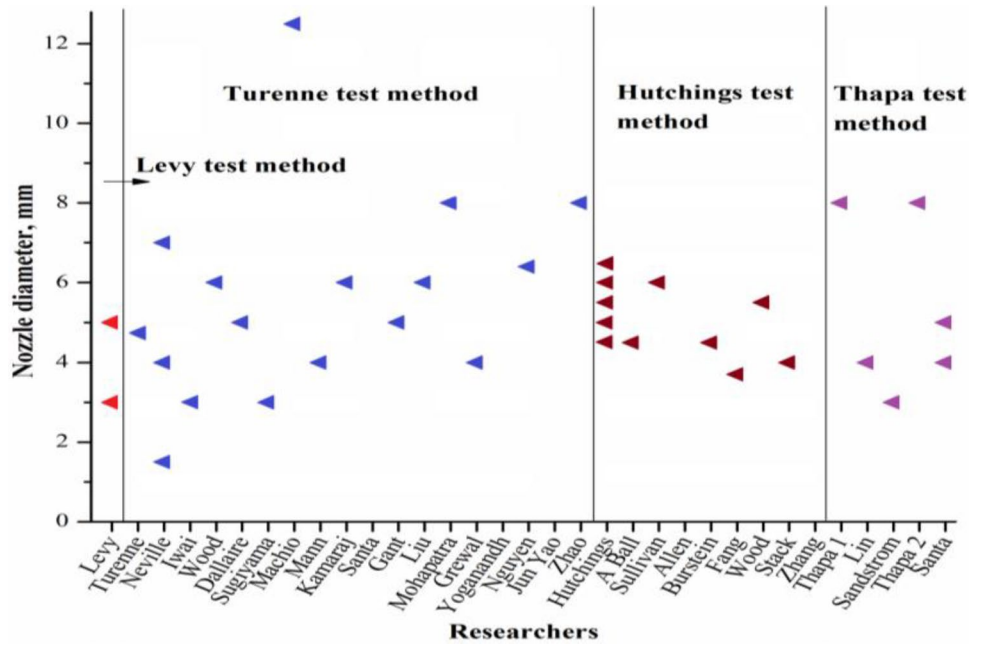
Fig. 6 Concentration comparison plot
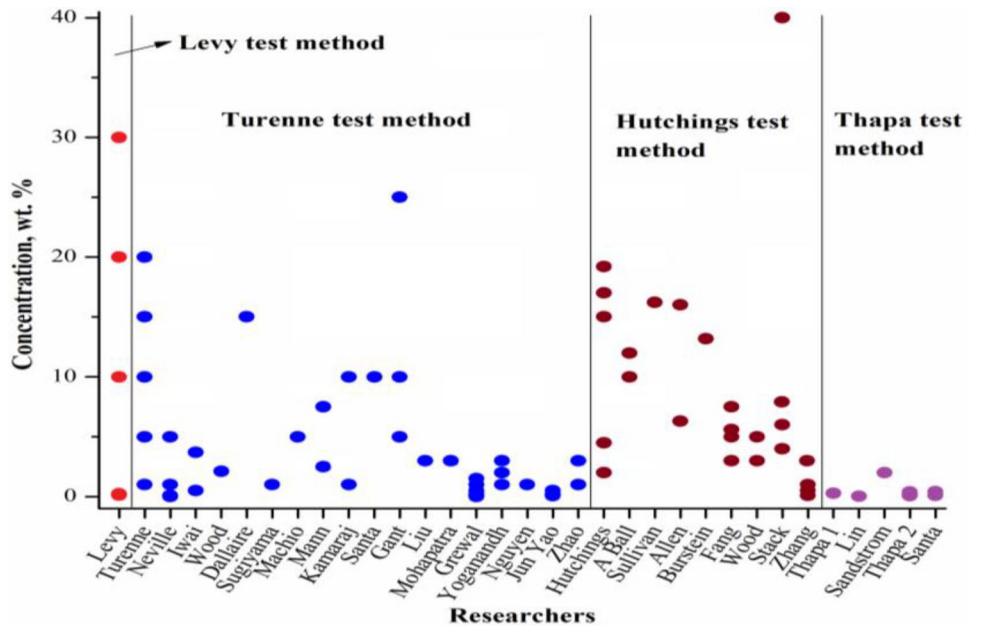
test set-ups built under Hutchings test method, mostly finds its usage for slurry transportation industries [30], marine industries [121], aircraft fields [112] while major research in this was carried to evaluate the material for synergy of erosion corrosion [112, 114, 118, 126, 130]. Under Thapa test method, test set-ups are built to evaluate the materials for hydraulic industries [31, 136, 138], while Levy test method is used for coal liquefaction industries [32]. It is observed from the literature that few researchers [29, 72, 81, 84, 98, 104] have not mentioned neither their objective of research either to develop a test set-up to test the material used for a

particular application, nor to test the material for its resistance to erosion. This makes difficult for the authors to have these test set-ups under any application. These test set-ups can only be discussed with the parameters used for the test set-ups. It is very obvious that the test parameters diverge considerably for the specific application.

Materials' erosion also depends on the type and size of erosive particles. Figure 7 shows the type of erosive particles comparison plot from all the classified test methods. It is observed from the literature that larger the size of particles, greater is the erosion damage on the materials and vice

versa. Erosion also depends on its shape, i.e., angular and rounded particles. Angular particles produced more erosion since it possessed sharp edges than the rounded particles. Larger the size of the particles, larger is the kinetic energy it possesses and greater is the erosion caused on the materials to evaluate the materials at severe conditions (Fig. 8).

Benefit of the slurry jet type set-ups is its ability to evaluate the test materials at various impingement angles ranging from 0° to 90°. Erosion mechanism of materials depends on the type of materials evaluated and on the angle of impingement. If the material is ductile, the mechanism will be in the micro ploughing (chip formation) or micro plastic deformation for lower angles, while micro cutting at higher angles. However, for brittle materials, it is micro fracture [3].

Based on the observations from Figs. 4, 6, and 7, the classified test methods based on velocity and concentration are further classified as low and high test method and are illustrated in Table 5. Table 5 also provides the details of RC and NRC type, premixed and postmixed methods, and the particle size employed in each classified test method.

5 Conclusions

Based on the research articles from the researchers on slurry jet erosion test set-up, the following conclusions can be made.

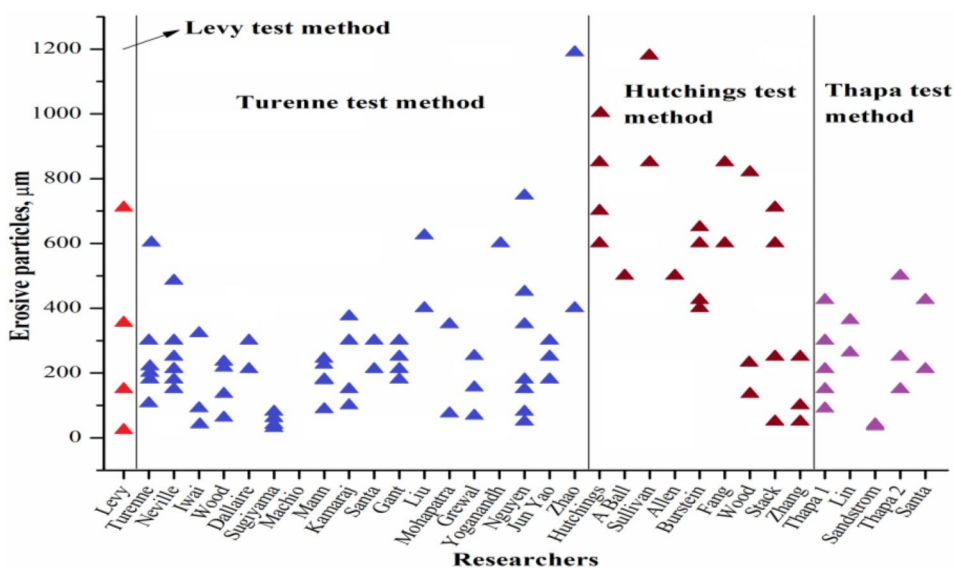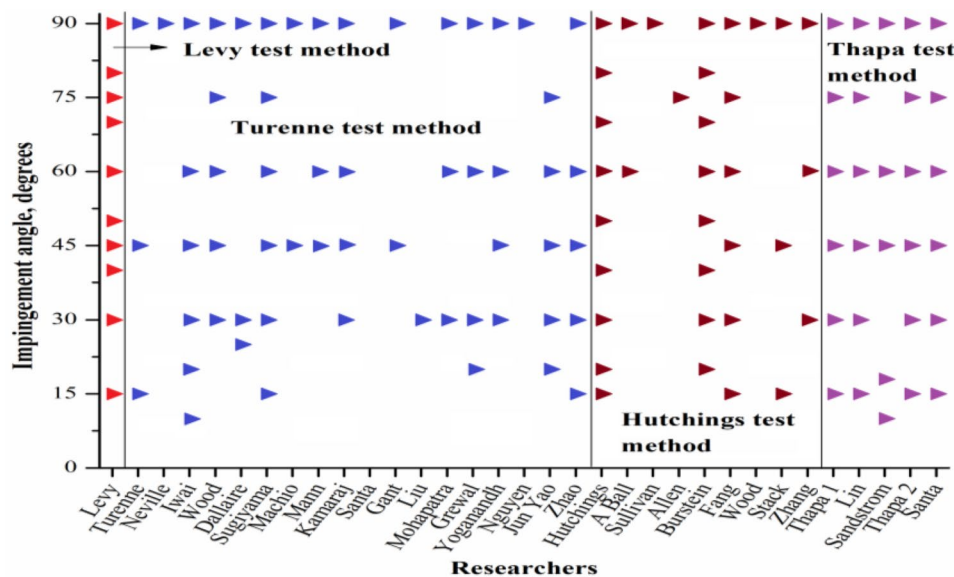**Fig. 7** Erosive particles comparison plot

Fig. 8 Impingement angle comparison plot

Table 5 Classification of test methods based on test parameters

Test method	RC/NRC	Premixed/postmixed	Velocity (m/s)		Concentration (wt%)		Particle size (µm)	
			Low	High	Low	High	Low	High
Levy	NRC	Premixed	8	38	0.12	30	24	710
Turenne	RC	Premixed	4	70	0.005	25	30	1190
Hutchings	RC	Post mixed	1.5	11	0.1	40	50	1180
Thapa	NRC	Postmixed	21	117.3	0.0015	2	35	500

- Based on the approach of the researchers for building the jet erosion test set-up, it is classified as Levy, Turenne, Hutchings, and Thapa test method, named after the original inventors.
- Based on the particle induction, test set-ups are classified as premixed and postmixed category and circulating (RC) and nonrecirculating (NRC) type.
- Levy and Turenne test method falls under premixing type, Hutching, and Thapa test method falls under postmixing category.
- Turenne test method is found to be the most popular test method; while Levy test method is less popular, based on the number of researchers adopted the test method.
- Erosion of the materials in the test set-up depends on velocity, concentration, and particles' size, shape, and kinetic energy
- Thapa test method is with highest of the velocity (117.3 m/s) but with lower concentration (0.0015 wt%) compared to all other test methods, while Hutchings test method is with highest concentration (40 wt%).
- Impingement angle in jet erosion test set-up is varied between 0° and 90°. Brittle materials showed higher erosion at 90° (brittle erosion), while ductile materials at 30° (ductile erosion).

Compliance with Ethical Standards

References

1. Tabor D (1969) Frank Philip Bowden. 1903–1968. Biogr Mem Fellows R Soc 15:1–38
2. Finnie I (1995) Some reflections on the past and future of erosion. Wear 186–187:1–10
3. Finnie I (1960) Erosion of surfaces by solid particles. Wear 3:87–103
4. Finnie I (1962) Erosion by solid particles in a fluid stream. In: Symposium on erosion and cavitation. ASTM International, West Conshohocken, pp 70–82
5. Greenwood NN, Spink JA (2003) An antipodean laboratory of remarkable distinction. Notes Rec R Soc 57:85–105
6. Bowden FP, Brunton JH (1958) Damage to solids by liquid impact at supersonic speeds. Nature 181:873–875
7. Bowden FP, Field JE (1964) The brittle fracture of solids by liquid impact, by solid impact, and by shock. Proc R Soc Lond A 282(1390):331–352
8. Finnie I (1972) Some observations on the erosion of ductile metals. Wear 19(1):81–90
9. Finnie I (1970) Study of the mechanisms of sand and dust erosion. Technical report, Solar Number RDR 1625-7. Air Mobility Research and Development Laboratory, Fort Eustis
10. Finnie I, Wolak J, Kabil Y (1967) Erosion of metals by solid particles. Materials 2:682
11. Adler WF (1979) Assessment of the state of knowledge pertaining to solid particle erosion. ETI-CR79-680. Effects Technology, Inc., Santa Barbara
12. Hutchings I, Shipway P (2017) Tribology: friction and wear of engineering materials. Butterworth-Heinemann, Oxford, p 189
13. Walley SM, Field JE (2005) The contribution of the Cavendish Laboratory to the understanding of solid particle erosion mechanisms. Wear 258:552–566
14. Kumar A, Sapra PK, Bhandari S (2011) A review paper on slurry erosion of plasma and flame thermal sprayed coatings. In: National conference on advancements and futuristic trends in mechanical and materials engineering, pp 1–5
15. Singla MK, Singh H, Chawla V (2011) Thermal sprayed CNT reinforced nanocomposite coatings—a review. Miner Mater Charact Eng 10(8):717–726
16. Wood RJK, Wheeler DW (1998) Design and performance of a high velocity air–sand jet impingement erosion facility. Wear 220(2):95–112
17. Compton WA, Steward KP (1968) Dust erosion of compressor materials: experience and prospects. In: ASME gas turbine conference and products show, Washington, DC, USA, pp 1–8
18. Mann BS, Arya V (2002) An experimental study to correlate water jet impingement erosion resistance and properties of metallic materials and coatings. Wear 253(5–6):650–661
19. Judkins RR, Bradley RA (1987) Erosion research on the US Department of Energy Fossil Energy Materials Program. In: ASME international gas turbine conference and exhibition, Anaheim, California, USA, pp 1–7
20. Blickensderfer R, Tylczak JH, Madsen BW (1985) Laboratory wear testing capabilities of the Bureau of Mines. US Department of the Interior, Bureau of Mines, pp 1–36
21. Rickerby DG, MacMillan NH (1980) The erosion of aluminum by solid particle impingement at normal incidence. Wear 60(2):369–382
22. Budinski KG (2007) Guide to friction, wear and erosion testing. ASTM International, West Conshohocken, pp 86–92

23. Kleis I, Kulu P (2007) Solid particle erosion: occurrence, prediction and control. Springer, London, pp 1–2

24. Summer RM (1987) A review of pipeline slurry erosion measurements and research recommendations. In: Miller JE, Schmidt FE (eds) Slurry erosion: uses, applications, and test methods, ASTM STP 946. American Society for Testing and Materials, Philadelphia, pp 91–100

25. Levy AV (1995) Solid particle erosion and erosion–corrosion of materials. ASM International, Cleveland, pp 1–2

26. Amarendra HJ, Chaudhari GP, Nath SK (2012) Synergy of cavitation and slurry erosion in the slurry pot tester. Wear 290:25–31

27. American Society for Testing and Materials (2000) ASTM Standard, G76-95, standard test method for conducting erosion tests by solid particle impingement using gas jets. American Society for Testing and Materials

28. Li SKK, Humphrey JA, Levy AV (1980) Erosive wear of ductile metals by a particle-laden high velocity liquid jet, LBL Report 11959. Materials and Molecular Research Division, Lawrence Berkeley Laboratory, University of California, Berkeley

29. Turenne S, Fiset M, Masounave J (1989) The effect of sand concentration on the erosion of materials by a slurry jet. Wear 133(1):95–106

30. Zu JB, Hutchings IM, Burstein GT (1990) Design of a slurry erosion test rig. Wear 140(2):331–344

31. Thapa B (2004) Sand erosion in hydraulic machinery. PhD Thesis, Norwegian University of Science and Technology, Norway

32. Li SKK, Humphrey JA, Levy AV (1981) Erosive wear of ductile metals by a particle-laden high velocity liquid jet. Wear 73(2):295–309

33. Levy AV, Yau P (1984) Erosion of steels in liquid slurries. Wear 98:163–182

34. Levy AV, Yan J, Arora VD (1985) Sand-water slurry erosion of carburized AISI 8620 steel. Wear 101:117–126

35. Mirza J, Turenne S, Masounave J (1990) Influence of structural parameters on abrasion–erosion resistance of various repairing mortars. Civ Eng 17:12–18

36. Turenne S, Chatigny Y, Simard D, Caron S, Masounave J (1990) The effect of abrasive particle size on the slurry erosion resistance of particulate-reinforced aluminium alloy. Wear 141:147–158

37. Turenne S, Simard D, Fiset M (1991) Influence of structural parameters on the slurry erosion resistance of squeeze-cast metal matrix composites. Wear 149:187–197

38. Turenne S, Fiset M (1993) Modeling of abrasive particle trajectories during erosion by a slurry jet. Wear 162:679–687

39. Neville A, Hodgkiess T, Dallas JT (1995) A study of the erosion–corrosion behaviour of engineering steels for marine pumping applications. Wear 186:497–507

40. Neville A, Hodgkiess T (1997) Study of effect of liquid corrosivity in liquid–solid impingement on cast iron and austenitic stainless steel. Br Corros J 32(3):197–205

41. Neville A, Hodgkiess T (1999) Characterisation of high-grade alloy behaviour in severe erosion–corrosion conditions. Wear 233:596–607

42. Hodgkiess T, Neville A, Shrestha S (1999) Electrochemical and mechanical interactions during erosion–corrosion of a high-velocity oxy-fuel coating and a stainless steel. Wear 233:623–634

43. Neville A, Reyes M, Hodgkiess T, Gledhill A (2000) Mechanisms of wear on a Co-base alloy in liquid–solid slurries. Wear 238(2):138–150

44. Neville A, Hu X (2001) Mechanical and electrochemical interactions during liquid–solid impingement on high-alloy stainless steels. Wear 251(1–12):1284–1294

45. Neville A, McDougall BAB (2001) Erosion– and cavitation–corrosion of titanium and its alloys. Wear 250(1–12):726–735

46. Reyes M, Neville A (2001) Mechanisms of erosion–corrosion on a cobalt-base alloy and stainless-steel UNS S17400 in aggressive slurries. J Mater Eng Perform 10(6):723–730

47. Neville A, McDougall BAB (2002) Electrochemical assessment of erosion–corrosion of commercially pure titanium and a titanium alloy in slurry impingement. Proc Inst Mech Eng L 216(1):31–41

48. Neville A, Reyes M, Xu H (2002) Examining corrosion effects and corrosion/erosion interactions on metallic materials in aqueous slurries. Tribol Int 35(10):643–650

49. Neville A, Hu X (2002) Assessment of electrochemical response from high alloy stainless steels during slurry impingement and single impacts to improve understanding of erosion–corrosion. Br Corros J 37(1):43–47

50. Malayoglu U, Neville A (2003) Comparing the performance of HIPed and Cast Stellite 6 alloy in liquid–solid slurries. Wear 255(1–6):181–194

51. De Souza VA, Neville A (2003) Corrosion and erosion damage mechanisms during erosion–corrosion of WC–Co–Cr cermet coatings. Wear 255(1–6):146–156

52. Hu X, Neville A (2005) The electrochemical response of stainless steels in liquid–solid impingement. Wear 258(1–4):641–648

53. Souza VAD, Neville A (2005) Corrosion and synergy in a WCCoCr HVOF thermal spray coating—understanding their role in erosion–corrosion degradation. Wear 259(1–6):171–180

54. Malayoglu U, Neville A (2005) Mo and W as alloying elements in Co-based alloys—their effects on erosion–corrosion resistance. Wear 259(1–6):219–229

55. Souza VAD, Neville A (2007) Aspects of microstructure on the synergy and overall material loss of thermal spray coatings in erosion–corrosion environments. Wear 263(1–6):339–346

56. Meng H, Hu X, Neville A (2007) A systematic erosion–corrosion study of two stainless steels in marine conditions via experimental design. Wear 263(1–6):355–362

57. Flores JF, Neville A, Kapur N, Gnanavelu A (2009) An experimental study of the erosion–corrosion behavior of plasma transferred arc MMCs. Wear 267(1–4):213–222

58. Flores JF, Neville A, Kapur N, Gnanavelu A (2009) Erosion–corrosion degradation mechanisms of Fe–Cr–C and WC–Fe–Cr–C PTA overlays in concentrated slurries. Wear 267(11):1811–1820

59. Flores JF, Neville A, Kapur N, Gnanavelu A (2011) Assessing the resistance of metal matrix composites and their microstructural integrity under erosion–corrosion. Wear 271(9–10):1331–1340

60. Iwai Y, Nambu K (1997) Slurry wear properties of pump lining materials. Wear 210:211–219

61. Wood RJK, Puget Y, Trethewey KR, Stokes K (1998) The performance of marine coatings and pipe materials under fluid-borne sand erosion. Wear 219:46–59

62. Wood RJK, Wheeler DW, Lejeau DC, Mellor BG (1999) Sand erosion performance of CVD boron carbide coated tungsten carbide. Wear 233:134–150

63. Wood RJK (1999) The sand erosion performance of coatings. Mater Des 20:179–191

64. Wheeler DW, Wood RJK (1999) Solid particle erosion of CVD diamond coatings. Wear 233:306–318

65. Wheeler DW, Wood RJK (2005) Erosion of hard surface coatings for use in offshore gate valves. Wear 258:526–536

66. Dallaire S (2001) Hard arc-sprayed coating with enhanced erosion and abrasion wear resistance. Therm Spray Technol 10(3):511–519

67. Dallaire S (2013) Slurry erosion resistance of boride-based overlays containing boride crystals oriented perpendicularly to the wearing surface. Wear 297:1006–1015

68. Sugiyama K, Nakahama S, Hattori S, Nakano K (2005) Slurry wear and cavitation erosion of thermal-sprayed cermets. Wear 258:768–775

69. Sugiyama K, Harada K, Hattori S (2008) Influence of impact angle of solid particles on erosion by slurry jet. Wear 265:713–720

70. Sugiyama K, Harada K, Hattori S (2008) Prediction of the volume loss by using slurry Jet Test on SCS6. Solid Mech Mater Eng 2(7):955–966

71. Machio CN (2005) Preparation, characterization and testing of WC-VC-CO HP/HV of thermal spray coatings. Doctoral Dissertation

72. Machio CN, Akdogan G, Witcomb MJ, Luyckx S (2005) Performance of WC–VC–Co thermal spray coatings in abrasion and slurry erosion tests. Wear 258:434–442

73. Mann BS, Arya V, Maiti AK, Rao MUB, Joshi P (2006) Corrosion and erosion performance of HVOF/TiAlN PVD coatings and candidate materials for high pressure gate valve application. Wear 260:75–82

74. Mann BS, Arya V, Pant BK (2013) High-power diode laser surface treated HVOF coating to combat high energy particle impact wear. Mater Eng Perform 22(7):1995–2004

75. Mann BS (2014) High-power diode laser-treated 13Cr4Ni stainless steel for hydro turbines. Mater Eng Perform 23(6):1964–1972

76. Manisekaran T, Kamaraj M, Sharrif SM, Joshi SV (2007) Slurry erosion studies on surface modified 13Cr–4Ni steels: effect of angle of impingement and particle size. Mater Eng Perform 16(5):567–572

77. Shivamurthy RC, Kamaraj M, Nagarajan R, Shariff SM, Padmanabham G (2009) Influence of microstructure on slurry erosive wear characteristics of laser surface alloyed 13Cr–4Ni steel. Wear 267:204–212

78. Shivamurthy RC, Kamaraj M, Nagarajan R, Shariff SM, Padmanabham G (2010) Slurry erosion characteristics and erosive wear mechanisms of Co-based and Ni-based coatings formed by laser surface alloying. Metall Mater Trans A 41A:470–486

79. Santa JF, Baena JC, Toro A (2007) Slurry erosion of thermal spray coatings and stainless steels for hydraulic machinery. Wear 263:258–264

80. Santa JF, Espitia LA, Blanco JA, Romo SA, Toro A (2009) Slurry and cavitation erosion resistance of thermal spray coatings. Wear 267:160–167

81. Gant AJ, Gee MG, Plint G (2007) A new concept in liquid jet erosion: commissioning and proving trials. Wear 263:284–288

82. Gant AJ, Gee MG (2009) Structure–property relationships in liquid jet erosion of tungsten carbide hard metals. Refract Met Hard Mater 27:332–343

83. Gant AJ, Gee MG (2015) Wear modes in slurry jet erosion of tungsten carbide hard metals: their relationship with microstructure and mechanical properties. Refract Met Hard Mater 49:192–202

84. Liu SL, Zheng XP, Geng GQ (2010) Influence of nano-WC–12Co powder addition in WC–10Co–4Cr AC-HVAF sprayed coatings on wear and erosion behavior. Wear 269:362–367

85. Randeep S, Mohapatra SK (2011) Study of the slurry erosion behaviour in hydropower plants. ME Thesis, Thapar University, India

86. Grewal HS, Bhandari S, Singh H (2012) Parametric study of slurry-erosion of hydroturbine steels with and without detonation gun spray coatings using Taguchi technique. Metall Mater Trans A 43A:3387–3401

87. Grewal HS, Agrawal A, Singh H (2013) Design and development of high-velocity slurry erosion test rig using CFD. Mater Eng Perform 22(1):152–161

88. Grewal HS, Singh H, Agrawal A (2014) A phenomenological model for slurry erosion prediction of thermal spray coatings. Tribol Lett 56:119–132

89. Grewal HS, Singh H, Agrawal A (2013) Slurry erosion mechanism of hydroturbine steel: effect of operating parameters. Tribol Lett 52:287–303

90. Grewal HS, Agrawal A, Singh H, Shollock BA (2014) Slurry erosion performance of Ni–Al₂O₃ based thermal-sprayed coatings: effect of angle of impingement. Therm spray Technol 23(3):389–401

91. Grewal HS, Singh H, Yoon ES (2015) Interplay between erodent concentration and impingement angle for erosion in dilute water–sand flows. Wear 332:1111–1119

92. Grewal HS, Arora HS, Singh H, Agrawal A, Mukherjee S (2014) Improving erosion resistance of hydroturbine steel using friction stir processing. Tribology 136:041102-1–41110

93. Grewal HS, Arora HS, Agrawal A, Singh H, Mukherjee S (2013) Slurry erosion of thermal spray coatings: effect of sand concentration. Procedia Eng 68:484–490

94. Yoganandh J, Natarajan S, Babu SK (2013) Erosive wear behavior of nickel-based high alloy white cast iron under mining conditions using Orthogonal Array. Mater Eng Perform 22(9):2534–2541

95. Yoganandh J, Natarajan S, Babu SK (2013) Erosion behaviour of WC–Co–Cr thermal spray coated grey cast iron under mining environment. Trans Indian Inst Met 66(4):437–443

96. Yoganandh J, Natarajan S, Kumaresh Babu SP (2014) Erosion behaviour of NiCrBSi coating under mining conditions. Surf Eng 30(1):71–77

97. Yoganandh J, Natarajan S, Babu SK (2015) Erosive wear behavior of high-alloy cast iron and duplex stainless steel under mining conditions. Mater Eng Perform 24(9):3588–3598

98. Nguyen VB, Nguyen QB, Liu ZG, Wan S, Lim CYH, Zhang YW (2014) A combined numerical–experimental study on the effect of surface evolution on the water–sand multiphase flow characteristics and the material erosion behavior. Wear 319:96–109

99. Nguyen QB, Lim CYH, Nguyen VB, Wan YM, Nai B, Zhang YW, Gupta M (2014) Slurry erosion characteristics and erosion mechanisms of stainless steel. Tribol Int 79:1–7

100. Nguyen VB, Nguyen QB, Zhang YW, Lim CYH, Khoo BC (2016) Effect of particle size on erosion characteristics. Wear 348:126–137

101. Zhao Y, Zhou F, Yao J, Dong S, Li N (2015) Investigation of erosion of stainless steel by two-phase jet impingement. Appl Therm Eng 88:353–362

102. Yao J, Zhou F, Zhao Y, Yin H, Guo Q, Li N (2015) Experimental investigation of erosion of stainless steel by liquid–solid flow jet impingement. Procedia Eng 102:1083–1091

103. Zhao Y, Zhou F, Yao J, Dong S, Li N (2015) Erosion–corrosion behavior and corrosion resistance of AISI 316 stainless steel in flow jet impingement. Wear 328:464–474

104. Zhao J, Ma A, Ji X, Jiang J, Bao Y (2018) Slurry erosion behavior of Al_xCoCrFeNiTi_{0.5} high-entropy alloy coatings fabricated by laser cladding. Metals 8:1–12

105. Wentzel EJ, Allen C (1997) The erosion–corrosion resistance of tungsten-carbide hard metals. Refract Met Hard Mater 15:81–87

106. Wood RJK, Wharton JA, Speyer AJ, Tan KS (2002) Investigation of erosion–corrosion processes using electrochemical noise measurements. Tribol Int 35:631–641

107. Stack MM, Pungwiwat N (2004) Erosion–corrosion mapping of Fe in aqueous slurries: some views on a new rationale for defining the erosion–corrosion interaction. Wear 256:565–576

108. Li Y, Burstein GT, Hutchings IM (1995) Influence of environmental composition and electrochemical potential on the slurry erosion–corrosion of aluminium. Wear 181–183:70–79

109. Bester JA (1993) The slurry erosive–corrosive wear of a selection of aluminium alloys, particulate reinforced aluminium metal matrix composites and a selection of steels. MS Thesis, University of Cape Town, South Africa

110. Zu JB, Burstein GT, Hutchings IM (1991) A comparative study of the slurry erosion and free-fall particle erosion of aluminium. Wear 149:73–84

111. Li Y, Burstein GT, Hutchings IM (1995) The influence of corrosion on the erosion of aluminium by aqueous silica slurries. Wear 186–187:515–522

112. Bester JA, Ball A (1993) The performance of aluminium alloys and particulate reinforced aluminium metal matrix composites in erosive–corrosive slurry environments. Wear 162–164:57–63

113. Lee-Sullivan P, Lu G (1994) Erosion of impact-notched holes in GFRP composites. Wear 176:81–88

114. Pugsley VA, Allen C (1999) Microstructure/property relationships in the slurry erosion of tungsten carbide–cobalt. Wear 225–229:1017–1024

115. Sasaki K, Burstein GT (1996) The generation of surface roughness during slurry erosion–corrosion and its effect on the pitting potential. Corros Sci 38(12):2111–2120

116. Burstein GT, Sasaki K (2000) Effect of impact angle on the slurry erosion–corrosion of 304L stainless steel. Wear 240:80–94

117. Fang Q, Sidky PS, Hocking MG (1997) The effect of corrosion and erosion on ceramic materials. Corros Sci 39(3):511–527

118. Fang Q, Sidky PS, Hocking MG (1998) Microripple formation and removal mechanism of ceramic materials by solid–liquid slurry erosion. Wear 223:93–101

119. Fang Q, Xu H, Sidky PS, Hocking MG (1999) Erosion of ceramic materials by a sand/water slurry jet. Wear 224:183–193

120. Fang Q, Sidky PS, Hocking GM (1999) Erosion resistance of continuously reinforced SiC–Ti-based metal matrix composites by a SiC/water slurry jet. Wear 233:174–181

121. Fang Q, Sidky PS, Hocking MG (1999) Erosion and corrosion of PSZ-zirconia and the t–m phase transformation. Wear 233–235:615–622

122. Tan KS, Wharton JA, Wood RJK (2005) Solid particle erosion–corrosion behaviour of a novel HVOF nickel aluminium bronze coating for marine applications—correlation between mass loss and electrochemical measurements. Wear 258:629–640

123. Barik RC, Wharton JA, Wood RJK, Tan KS, Stokes KR (2005) Erosion and erosion–corrosion performance of cast and thermally sprayed nickel–aluminium bronze. Wear 259:230–242

124. Wharton JA, Barik RC, Kear G, Wood RJK, Stokes KR, Walsh FC (2005) The corrosion of nickel–aluminium bronze in seawater. Corros Sci 47:3336–3367

125. Barik RC, Wharton JA, Wood RJK, Stokes KR (2009) Electro-mechanical interactions during erosion–corrosion. Wear 267:1900–1908

126. Stack MM, El-Badia TA (2008) Some comments on mapping the combined effects of slurry concentration, impact velocity and electrochemical potential on the erosion–corrosion of WC/Co–Cr coatings. Wear 264:826–837

127. Stack MM, Abdulrahman GH (2010) Mapping erosion–corrosion of carbon steel in oil exploration conditions: some new approaches to characterizing mechanisms and synergies. Tribol Int 43(7):1268–1277

128. Stack MM, Abdulrahman GH (2012) Mapping erosion–corrosion of carbon steel in oil–water solutions: effects of velocity and applied potential. Wear 274:401–413

129. Zhang GA, Xu LY, Cheng YF (2009) Investigation of erosion–corrosion of 3003 aluminum alloy in ethylene glycol–water solution by impingement jet system. Corros Sci 51:283–290

130. Saha GC, Khan TI, Zhang GA (2011) Erosion–corrosion resistance of microcrystalline and near-nanocrystalline WC–17Co high velocity oxy-fuel thermal spray coatings. Corros Sci 53:2106–2114

131. Sandstrom MJ (2003) The solid particle erosion of tungsten carbide in silicon carbide slurry. MS Thesis, University of Utah

132. Lin HC, Wu SK, Yeh CH (2001) A comparison of slurry erosion characteristics of TiNi shape memory alloys and SUS304 stainless steel. Wear 249:557–565

133. Thapa B, Shrestha R, Dhakal P, Thapa BS (2005) Sediment in Nepalese hydropower projects. In: Proceedings of the international conference on the Great Himalayas: climate, health, ecology, management and conservation, pp 251–258

134. Thapa BS, Thapa B, Dahlhaug OG (2012) Current research in hydraulic turbines for handling sediments. Energy 47:62–69

135. Poudel LP, Thapa B, Shrestha BP, Shrestha NK (2012) Impact of sand on hydraulic turbine material: a case study of Roshi Khola, Nepal. Hydro Nepal Water Energy Environ 10:60–65

136. Lin HC, Lin KM, Chen YS, Yang CH (2005) Ion nitriding of Fe–30Mn–6Si–5Cr shape memory alloy: II. Erosion characteristics. Surf Coat Technol 194:74–81

137. Lin MC, Chang LS, Lin HC, Yang CH, Lin KM (2006) A study of high-speed slurry erosion of NiCrBSi thermal-sprayed coating. Surf Coat Technol 201:3193–3198

138. Romo SA, Santa JF, Giraldo JE, Toro A (2010) High-velocity slurry erosion of welded cobalt-based alloys. In: First international Brazilian conference on tribology, pp 234–243

139. Romo SA, Santa JF, Giraldo JE, Toro A (2012) Cavitation and high-velocity slurry erosion resistance of welded Stellite 6 alloy. Tribol Int 47:16–24

140. Blau PJ (1992) ASM handbook, friction, lubrication, and wear technology, vol 18. ASM International, Cleveland

141. Helle A, Andersson P, Ahlroos T, Kupiainen V (2004) Erosive wear of coatings and methods to monitor coating wear—a literature study. Research Report No. BTUO43-041265

142. Mann BS (2015) Laser surface treatment of hydro and thermal power plant components and their coatings: a review and recent findings. Mater Eng Perform 24(11):4488–4502